Editors' Suggestion

Structural Relaxation Time of a Polymer Glass during Deformation

Pradip K. Bera,[1,*] Grigori A. Medvedev,[2] James M. Caruthers,[2] and Mark D. Ediger[1]
[1]University of Wisconsin-Madison, Madison, Wisconsin 53706, USA
[2]Purdue University, West Lafayette, Indiana 47907, USA

(Received 9 December 2023; accepted 18 April 2024; published 15 May 2024)

In order to determine the structural relaxation time of a polymer glass during deformation, a strain rate switching experiment is performed in the steady-state plastic flow regime. A lightly cross-linked poly (methylmethacrylate) glass was utilized and, simultaneously, the segmental motion in the glass was quantified using an optical probe reorientation method. After the strain rate switch, a nonmonotonic stress response is observed, consistent with previous work. The correlation time for segmental motion, in contrast, monotonically evolves toward a new steady state, providing an unambiguous measurement of the structural relaxation time during deformation, which is found to be approximately equal to the segmental correlation time. The Chen-Schweizer model qualitatively predicts the changes in the segmental correlation time and the observed nonmonotonic stress response. In addition, our experiments are reasonably consistent with the material time assumption used in polymer deformation modeling; in this approach, the response of a polymer glass to a large deformation is described by combining a linear-response model with a time-dependent segmental correlation time.

DOI: 10.1103/PhysRevLett.132.208101

Introduction.—Polymer glasses play an important role in our modern life as flexible, transparent, light, and easily processable industrial materials. As glasses, their nonequilibrium nature is fundamental and the glass slowly evolves toward an equilibrium structure [1]. This slow structural evolution of the glass is limited by the rate of molecular rearrangements and occurs at a rate that depends on the temperature, pressure, chemical composition, and thermobaric history [2]. "Physical aging" describes the changes in physical properties that occur as result of this evolution, for example, the viscoelastic shear modulus typically increases during aging [3]. Notably, physical aging does not involve any chemical change, and it can be completely reversed by heating the sample above the glass transition temperature, in a process known as thermal rejuvenation. Even with no temperature change, other external stimuli such as shear or tensile deformation can also reverse (some of) the effects of physical aging [4,5]. At a qualitative level, one can envision the physical aging of glass as the system moving lower on the potential energy landscape (PEL) where the barriers to rearrangement are higher, while thermal or mechanical rejuvenation can be envisioned as moving up the PEL to where the barriers are lower [6–9].

One of the most important quantities for understanding a glass-forming system is the structural relaxation time [10–15]. To obtain this quantity, often a small temperature jump (either positive or negative) is applied to drive the system from the equilibrium liquid at T_1 to the equilibrium liquid at T_2 [16,17]. It has been established that the density, modulus, and molecular mobility of a glass all change monotonically in response to such a temperature jump, and all these quantities reach their new equilibrium values at about the same time [18,19]. To a reasonable approximation, the equilibration time for any of these quantities can be used to determine the structural relaxation time, which can be envisioned as the characteristic time to move between two levels on the PEL [20]. Recent work has made extensive comparisons between the structural relaxation time (measured through a small temperature jump) and underlying molecular motion in the equilibrium liquid [17,21–25], with the conclusion that, in absence of other external stimuli such as shear or tensile deformation, the primary (α) process of the equilibrium liquid controls the observed structural relaxation, at least so long as the temperature jump is small. In qualitative terms, for quiescent polymeric systems, this establishes that segmental rearrangements control the physical aging process.

Here, we measure the structural relaxation time of a polymer glass *during* tensile deformation. When a polymer glass is subjected to mechanical forces, as happens in many critical applications, the structure of the glass and the position on the PEL can evolve in response. Many theoretical efforts attempt to describe this complex process, often in the form of constitutive equations. As all current approaches appear to have deficiencies [26,27], we attempt here to advance our understanding through an analogy with the temperature jump experiments described above. Generalizing, we define the structural relaxation time of a polymer glass during deformation as the time required for the isothermal transition from one mechanical steady state to another. Nanzai performed such an experiment on a

PMMA glass [28], making use of the plastic flow regime that occurs after yield during mechanical deformation at a constant strain rate. Once a steady-state (constant stress) flow had been established, the strain rate was quickly switched. Interestingly, a stress undershoot appeared when the strain rate was decreased by 2 orders of magnitude. Unfortunately, this nonmonotonic response of the stress creates significant ambiguity for a determination of the structural relaxation time. Furthermore, there is no consensus on the interpretation of this striking stress undershoot. Recently, Medvedev and Caruthers investigated a series of theoretical models and found that several models failed to produce the stress undershoot after strain rate switching, while other models could qualitatively reproduce the experimental observations [29].

Here we revisit Nanzai's strain rate switching experiment with a new tool: the measurement of the segmental correlation time τ_{seg} during deformation. Recent experiments and simulations have shown that the segmental dynamics of the polymer glass are intimately connected with the deformation response [30–33]. As the polymer glass yields and flows, the segmental correlation time is reduced by an order of magnitude or more. Qualitatively, deformation turns a solid into a liquid, by increasing the rate of segmental relaxation until it is comparable to the deformation rate. This fundamental connection between the polymer segmental correlation time and deformation is embedded in almost all theoretical models through the use of the concept of material time [34,35]. With this approach, the response of a polymer glass to a large deformation can be captured by the model describing the linear-response regime, except that the segmental correlation time becomes a time-dependent variable that is altered by the deformation [35]. Though widely used, the validity of the material time approximation is unclear.

Results.—In this Letter, we mechanically induce a isothermal, steady-state to steady-state transition of the PMMA polymer glass at 380 K, i.e., $T_g - 19$ K. We apply a constant strain rate to deform the PMMA glass and wait until it reaches steady state in the flow regime. Then, we impose an order of magnitude switch to the applied strain rate and wait again for the material response to reach the new steady state. We follow the local strain rate ($\dot{\gamma}_{\mathrm{locl}}$) and the segmental dynamics *in situ*, in order to measure the structural relaxation time of the polymer glass as it responds to the strain rate switch. Additional experimental details may be found in Supplemental Material [36]. The anisotropy decay after photobleaching due to the reorientation of the N,N′-dipentyl-3,4,9,10-perylenedicarboximide probe has previously been shown to be an excellent reporter of the segmental dynamics of PMMA [37–39]. The timescale τ_{seg} extracted by the Kohlrausch-Williams-Watts (KWW) function fitting to the anisotropy decay is a measure of the timescale of the PMMA segmental dynamics.

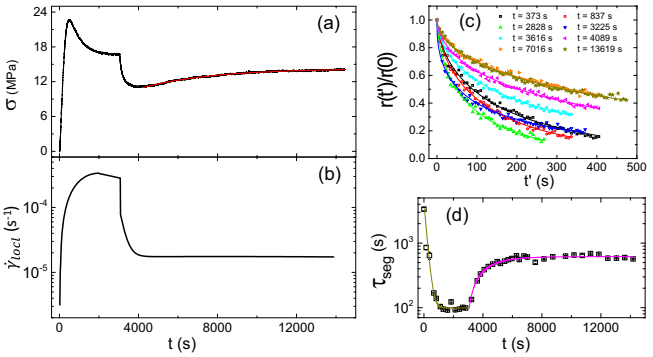

FIG. 1. High-to-low strain rate switching experiment (switching from 6×10^{-5} to 6×10^{-6} s^{-1} at $t = 3075$ s). (a) Time dependence of measured stress σ; along with the functional fit $Y = Y_s + (Y_i - Y_s)\exp[-(t - t_0)/\tau_Y]$ starting after the minimum at 4000 s, shown in red. The fitted transition time is $\tau_\sigma = 3760 \pm 160$ s. (b) Measured local strain rate; $\dot{\gamma}_{\mathrm{locl}}$ is plotted with t. (c) A subset of the normalized anisotropy decay curves $r(t')/r(0)$, measured at various times t after the start of deformation, are shown as examples. Solid lines are KWW fits. (d) The segmental correlation time τ_{seg} extracted from the KWW fits are plotted vs time t. Error bars show fitting errors. Solid curves are similar functional fits as in (a) with $\tau_{\tau\text{-seg}} = 165 \pm 10$ for the green curve and $\tau_{\tau\text{-seg}} = 1330 \pm 110$ for the magenta curve.

We first describe the high-to-low strain rate switching experiment. We set $t = 0$ s at the start of sample deformation, i.e., after the 36 min aging. We initially applied the global strain rate $\dot{\epsilon} = 6 \times 10^{-5}$ s^{-1} until $t = 3075$ s, and then we had switched to $\dot{\epsilon} = 6 \times 10^{-6}$ s^{-1}. The measured global stress σ (= [measured force/(2.3 mm × 50 μm)]) is plotted against the duration of the experiment in Fig. 1(a). We can observe an initial linear region due to elasticity, then yielding with maximum $\sigma \approx 22.6$ MPa, followed by strain softening, and then a steady state (≈17 MPa) until 3075 s. After switching the strain rate, σ shows a minimum around 4000 s, and then goes to the second steady state ≈14.5 MPa. The extracted timescale for σ to reach the steady state after the minimum is $\tau_\sigma = 3760 \pm 160$ s. The observed behavior of σ following the strain rate drop is in qualitative agreement with Nanzai's compressive experiment with PMMA [28]. The measured local strain rate $\dot{\gamma}_{\mathrm{locl}}$ does not immediately switch to the lower value. Instead, it takes ∼1000 s [Fig. 1(b)] to make a monotonic transition from the first steady-state strain rate ($\approx 3 \times 10^{-4}$ s^{-1}) to the second steady-state strain rate ($\approx 2 \times 10^{-5}$ s^{-1}). We stopped this experiment at 14000 s. We then reversed the linear actuator back to the initial position and thermally rejuvenated the sample to erase history, enabling further measurements with the same sample.

We repeated this high-to-low strain rate switching experiment two additional times, in order to perform fluorescence anisotropy measurements at several time points during the transition between steady states. The global stresses for these three experiments are in excellent

agreement, confirming the repeatability of the experiment (Supplemental Material Fig. S2 [36]). A subset of the anisotropy decay curves are shown in Fig. 1(c), along with fits to the KWW function. The extracted segmental correlation time (τ_{seg}) from each anisotropy curve is plotted against deformation time (t) in Fig. 1(d), at the time corresponding to the midpoint of the anisotropy decay measurement. We observe an order of magnitude decrease in τ_{seg} (from ≈3300 to ≈100 s) due to yielding. After strain rate switching, there is a monotonic increase in τ_{seg} to reach the second steady state ($\tau_{seg} \approx 620$ s). In Fig. 1(d), we show fitted curves that reproduce the variations of τ_{seg} with two different functions used before and after switching. For the steady-state to steady-state transition, the extracted timescale for the change in τ_{seg} is $\tau_{\tau\text{-seg}} = 1330 \pm 110$ s which is significantly $< \tau_\sigma$, the timescale of σ.

With this same sample, we have also performed low-to-high strain rate switching experiment, switching from $\dot{\epsilon} = 6 \times 10^{-6}$ to $\dot{\epsilon} = 6 \times 10^{-5}$ s^{-1}. In this case, σ shows an overshoot at $t = 17\,300$ s [Fig. 2(a)] having very nearly the same maximum value as in Fig. 1(a) before transitioning to the second steady state at $t \sim 17\,800$ s. The local strain rate ($\dot{\gamma}_{locl}$) goes to the second steady state at $t \sim 17900$ s [Fig. 2(b)]. Again a subset of the anisotropy decay curves measured during this experiment are shown in Fig. 2(c). The decay curve observed immediately after switching cannot be well described by the KWW function; this will be discussed below. When the strain rate suddenly switched, the extracted τ_{seg} values decrease and then become steady at $t \sim 17\,800$ s [Fig. 2(d)]. In this case, all the three measured quantities σ, $\dot{\gamma}_{locl}$, and τ_{seg} reach the steady state so quickly that we cannot meaningfully distinguish their transition times. Fits capturing the variations in τ_{seg} are shown before ($\tau_{\tau\text{-seg}} = 2365 \pm 85$ s) and after ($\tau_{\tau\text{-seg}} = 200 \pm 45$ s) the switching.

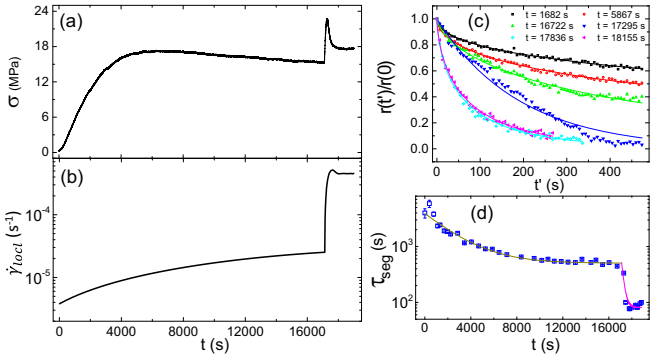

FIG. 2. Low-to-high strain rate switching experiment (switching from 6×10^{-6} to 6×10^{-5} s^{-1} at $t = 17114$ s). Variations of σ, $\dot{\gamma}_{locl}$, a few $r(t')/r(0)$, and τ_{seg} are shown in (a)–(d) respectively. Error bars are fitting errors. Solid curves in (d) are the functional fits $Y = Y_s + (Y_i - Y_s)\exp[-(t - t_0)/\tau_Y]$ with timescales $\tau_{\tau\text{-seg}} = 2365 \pm 85$ s for the green curve and $\tau_{\tau\text{-seg}} = 200 \pm 45$ for the magenta curve.

During the strain rate switching experiments, there are significant changes in the KWW nonexponentiality parameter β [42]. For a system at steady state, β can be interpreted in terms of a distribution of segmental correlation times (the characteristic length scale for dynamic heterogeneity is a few nanometers). β has limits $0 < \beta < 1$, where smaller values of β indicate a broader distribution of correlation times. Deformation has been previously reported to narrow the distribution of the segmental correlation time within a polymer glass [31,43]. Here, for both types of strain rate switching experiments, β increases from 0.4 to a steady value in the range of 0.6–0.7, depending upon the applied strain rate (Supplemental Material Fig. S3 [36]). This is consistent with previous studies [44]. After the strain rate switching, β transitions from one steady-state value to another, with anomalous KWW β parameters being obtained immediately after the switch. These anisotropy curves are not well described by the KWW function and are further discussed below.

In order to further analyze our results, we test whether our anisotropy decay curves are consistent with the material time approximation (i.e., $\beta \sim$ constant) [24,34]. Models that make this approximation typically couple the mechanical response expected in the linear-response regime with a variable clock rate that accounts for the effects of nonlinear deformation. If this approximation is valid, the anisotropy decay functions that show substantial variation in Figs. 1(c) and 2(c) would all superpose when viewed as a function of material time. We use the observed time variations of τ_{seg}, i.e., the fitted curves in Figs. 1(d) and 2(d), to calculate the variation of material time (ξ) with respect to the real time (t) using $\xi = \int_0^t (\tau_u/\tau_{seg})dt'$, where τ_u is the value of τ_{seg} before starting the deformation [24]. In Figs. 3(a) and 3(c), ξ is plotted with respect to t, respectively.

Remarkably, when we look at all the anisotropy decay curves in terms of material time, all the decay curves overlap well, including the decay curve just before deformation [Figs. 3(b) and 3(d)]. This agreement also includes the decay curves observed immediately after strain rate switching which were poorly fit using the KWW function (Supplemental Material Fig. S4 [36]). The nonlinear variation of material time shifts the data points of decay curves in such a way that all the decay curves fall close to the undeformed one. As discussed above, material time is a common assumption in models of polymer deformation and these results indicate that it is a reasonable approximation for the deformations considered here.

We can now address the following questions regarding our high-to-low strain rate switching data: (1) Can we determine and understand the structural relaxation time for the PMMA glass for the transition between the two steady-state flow regimes? (2) Why does σ show an undershoot after switching to a low strain rate, whereas the segmental correlation times τ_{seg} increase monotonically?

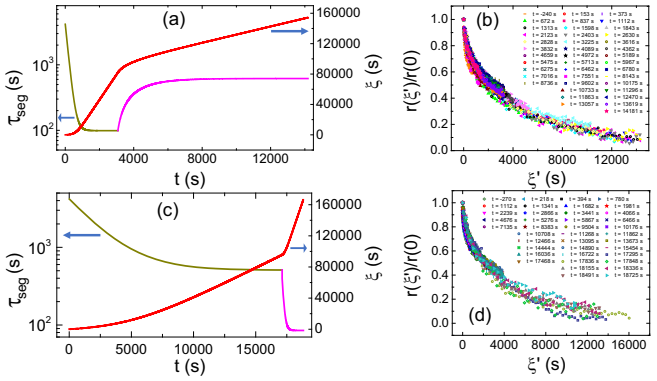

FIG. 3. Experimental time vs material time: (a),(c) The variation of τ_{seg} vs t during the full span of the experiments [fitted data from Figs. 1(d) and 2(d)] is shown along with the calculated material time. (b),(d) Normalized anisotropy decay curves for the two types of experiments are replotted. In material time, ξ' is used to denote elapsed material time since the beginning of an anisotropy measurement.

To address these questions, we compare our data to the nonlinear Langevin equation theory proposed by Chen and Schweizer [40,45–47]. In this approach, a structural state variable S_0, related to the amplitude of density fluctuations on the nanometer scale, controls the response of the glass to deformation. Figures 4(a)–4(c) show the predictions of the Chen-Schweizer model for the strain rate switching experiment for S_0, the stress σ, and the segmental correlation time τ_{seg} (see Supplemental Material for details about the model calculations [36]). All of the qualitative features of the experiments are well described by the model calculations. In particular, the predicted variations of both σ and τ_{seg} resemble the experimental observations of strain rate switching. We have extracted the characteristic relaxation times τ_σ, $\tau_{\tau\text{-seg}}$, and τ_S associated with the variations of the parameters σ, τ_{seg}, and S_0, respectively (Supplemental Material Fig. S5 [36]), in a manner analogous to our treatment of the experimental data.

To address the first question, regarding experimental access to the structural relaxation time for the transition from one steady-state flow to another, we observe that $\tau_{\tau\text{-seg}} \approx \tau_S$. This was also noted by Chen and Schweizer [40]

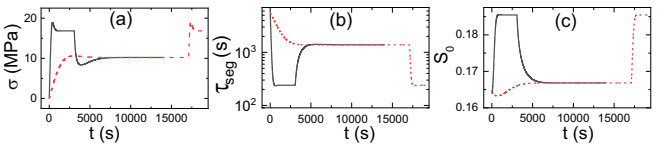

FIG. 4. Chen-Schweizer model predictions for strain rate switching experiments on PMMA glass, using the global strain rates 6×10^{-5} and 6×10^{-6} s^{-1} as inputs. Model outputs are the time variation of (a) the stress σ, (b) the segmental correlation time τ_{seg}, and (c) the structural state variable S_0. Black curves are for high-to-low strain rate switching, and dotted red lines are for low-to-high strain rate switching.

and within the context of the model, τ_S is the structural relaxation time. So the experimental observation of $\tau_{\tau\text{-seg}}$ provides a reasonable estimate of the τ_S in case of steady-state to steady-state transition of flow of polymer glass. To verify the generality of this conclusion, we performed calculations with a less complex model ("toy model 1" from Ref. [48]). Similar to the Chen-Schweizer model, we observed that the state variable and τ_{seg} approached steady state on a similar timescale. Furthermore, both our results and the Chen-Schweizer model indicate that the structural relaxation time during deformation is very similar to the segmental correlation time itself. Thus, our Letter extends the connection between segmental mobility and structural relaxation from the quiescent state (where it is well established) to a mechanically driven steady state.

With regard to the second question, we can address why σ shows an undershoot after switching to a low strain rate, whereas the segmental correlation time τ_{seg} increases monotonically. The model successfully reproduces the experimental observation of slower variation of σ compared to τ_{seg}, i.e., $\tau_\sigma > \tau_{\tau\text{-seg}}$. To get a detailed understanding of the undershoot in σ, we have done additional numerical calculations with the model equations in which we keep the τ_{seg} and S_0 precisely fixed after the τ_{seg} has very nearly reached its steady-state value. Under these conditions, σ continues to vary for a considerable length of time, mainly controlled by the second term of the generalized Maxwell constitutive equation in the Chen and Schweizer model [47], i.e., $-(\sigma/\tau_{\mathrm{seg}})$ as $\sigma \ll \sigma_c$ [Supplemental Material Eq. (1), Fig. S6 [36]]. This lag in the stress response was also pointed out by Nanzai [28]. Within the Chen and Schweizer model, this interpretation is possible: the undershoot occurs when a system high in the landscape (as a result of fast deformation) suddenly experiences slower deformation; the stress naturally drops when the strain rate goes down, but it takes some time (roughly τ_S) for the system to "age" down to its new position in the landscape. As the system ages, the barriers to relaxation grow, and thus the stress must increase in order to maintain the strain rate.

We see two important directions for extending this Letter. Similar experiments further below T_g would test the generality of our results. Recent work [44] has shown that the segmental correlation time of a deformed polymer glass in the flow regime is a weak function of temperature, for a given strain rate. We anticipate that, at lower temperatures, the structural relaxation time during deformation continues to be controlled by the (deformation-accelerated) segmental mobility. Together, these two observations suggest that strain rate switching experiments further below T_g will be qualitatively similar to the ones shown here. Additionally, there is a need for better models to describe the deformation of polymer glasses. Most models of polymer glass deformation do not describe the distribution of correlation times known to be important in glassy systems [29]. The Chen-Schweizer approach has recently

been extended to account for heterogeneous dynamics [49]. The increase of the KWW β parameter with increasing strain rate (as seen here and previously [44]) is at least qualitatively accounted for in the new work.

Summary.—To measure the structural relaxation time for a polymer glass during deformation, we have performed strain rate switching measurements on a PMMA glass at $T_g - 20$ K. In addition to observing the resulting stress, we have measured the time variation of the segmental correlation time of the polymer. We have shown that the correlation functions describing segmental mobility are approximately invariant when plotted in material time. This result supports the use of material time in models of polymer glass deformation. The Chen-Schweizer model qualitatively describes the evolution of the stress and segmental correlation time for the strain rate switching experiments. It allows an interpretation of the undershoot of the stress in terms of the energy landscape. Our optical experiments indicate that the structural relaxation time during deformation is very similar to the segmental correlation time itself. Thus, our Letter extends the connection between segmental mobility and structural relaxation from the quiescent state to a mechanically driven steady state.

G. A. M. and J. M. C. acknowledge support from National Science Foundation Grant No. 1761610-CMMI. P. K. B. and M. D. E. acknowledge support from the National Science Foundation (DMR) Grant No. DMR-2002959.

*pbera2@wisc.edu

[1] I. M. Hodge, Physical aging in polymer glasses, Science **267**, 1945 (1995).
[2] M. D. Ediger, C. A. Angell, and S. R. Nagel, Supercooled liquids and glasses, J. Phys. Chem. **100**, 13200 (1996).
[3] C. E. L. Struik, *Physical Aging in Amorphous Polymers and Other Materials* (Elsevier, Oxford, 1978), Vol. 106.
[4] A. D. Parmar, S. Kumar, and S. Sastry, Strain localization above the yielding point in cyclically deformed glasses, Phys. Rev. X **9**, 021018 (2019).
[5] M. O. R. Mota, E. T. Lund, S. Sohn, D. J. Browne, D. C. Hofmann, S. Curtarolo, A. van de Walle, and J. Schroers, Enhancing ductility in bulk metallic glasses by straining during cooling, Commun. Mater. **2**, 23 (2021).
[6] G. B. McKenna, Mechanical rejuvenation in polymer glasses: Fact or fallacy?, J. Phys. Condens. Matter **15**, S737 (2003).
[7] E. Yang and R. A. Riggleman, Role of local structure in the enhanced dynamics of deformed glasses, Phys. Rev. Lett. **128**, 097801 (2022).
[8] R. A. Riggleman, K. S. Schweizer, and J. J. d. Pablo, Nonlinear creep in a polymer glass, Macromolecules **41**, 4969 (2008).
[9] A. Y. H. Liu and J. Rottler, Aging under stress in polymer glasses, Soft Matter **6**, 4858 (2010).
[10] A. J. Kovacs, "Transition vitreuse dans les polymères amorphes" in etude phénoménologique, Adv. Polymer Sci. **3**, 394 (1964).
[11] G. Scherer, *Relaxation in Glass and Composites* (Wiley-Interscience, New York, 1986).
[12] J. Málek and J. Shánělová, *Properties and Applications of Amorphous Materials* (Kluwer Academic Publishers, London, 2001), pp. 35–44.
[13] R. D. Priestley, C. J. Ellison, L. J. Broadbelt, and J. M. Torkelson, Structural relaxation of polymer glasses at surfaces, interfaces, and in between, Science **309**, 456 (2005).
[14] A. D. Parmar, P. Kundu, and S. Sastry, Density dependence of relaxation dynamics in glass formers, and the dependence of their fragility on the softness of inter-particle interactions, J. Chem. Sci. **129**, 1081 (2017).
[15] M. Adhikari, S. Karmakar, and S. Sastry, Dependence of the glass transition and jamming densities on spatial dimension, Phys. Rev. Lett. **131**, 168202 (2023).
[16] R. Richert, Supercooled liquids and glasses by dielectric relaxation spectroscopy, Adv. Chem. Phys. **156**, 101 (2014).
[17] R. Richert, One experiment makes a direct comparison of structural recovery with equilibrium relaxation, J. Chem. Phys. **157**, 224501 (2022).
[18] T. Hecksher, N. B. Olsen, and J. C. Dyre, Communication: Direct tests of single-parameter aging, J. Chem. Phys. **142**, 241103 (2015).
[19] T. Hecksher, N. B. Olsen, and J. C. Dyre, Fast contribution to the activation energy of a glass-forming liquid, Proc. Natl. Acad. Sci. U.S.A. **116**, 16736 (2019).
[20] T. Ekimoto, A. Yoshimori, T. Odagaki, and T. Yoshidome, A theoretical framework for calculations of the structural relaxation time on the basis of the free energy landscape theory, Chem. Phys. Lett. **577**, 58 (2013).
[21] T. Hecksher, N. B. Olsen, K. Niss, and J. C. Dyre, Physical aging of molecular glasses studied by a device allowing for rapid thermal equilibration, J. Chem. Phys. **133**, 174514 (2010).
[22] J. E. Schawe, Vitrification in a wide cooling rate range: The relations between cooling rate, relaxation time, transition width, and fragility, J. Chem. Phys. **141**, 184905 (2014).
[23] M. K. Saini, X. Jin, T. Wu, Y. Liu, and L. M. Wang, Interplay of intermolecular interactions and flexibility to mediate glass forming ability and fragility: A study of chemical analogs, J. Chem. Phys. **148**, 124504 (2018).
[24] V. Di Lisio, V. M. Stavropoulou, and D. Cangialosi, Physical aging in molecular glasses beyond the α relaxation, J. Chem. Phys. **159**, 064505 (2023).
[25] S. Lapuk, M. Ponomareva, M. Ziganshin, R. Larionov, T. Mukhametzyanov, C. Schick, and I. Lounev, A. Gerasimov, Some aspects of the glass transition of polyvinylpyrrolidone depending on the molecular mass, Phys. Chem. Chem. Phys. **25**, 10706 (2023).
[26] L. Anand and N. Ames, On modeling the micro-indentation response of an amorphous polymer, Int. J. Plast. **22**, 1123 (2006).
[27] L. Van Breemen, E. Klompen, L. Govaert, and H. Meijer, Extending the EGP constitutive model for polymer glasses to multiple relaxation times, J. Mech. Phys. Solids **59**, 2191 (2011).

[28] Y. Nanzai, Transition mechanism from elastic deformation to plastic flow in poly(methylmethacrylate), Polym. Eng. Sci. **30**, 96 (1990).
[29] G. A. Medvedev and J. M. Caruthers, in *A Comparison of Constitutive Descriptions of the Thermo-Mechanical Behavior of Polymeric Glasses" in Polymer Glasses*, edited by C. B. Roth (Taylor & Francis Books, London, 2016), pp. 451–536.
[30] H. N. Lee, K. Paeng, S. F. Swallen, and M. Ediger, Dye reorientation as a probe of stress-induced mobility in polymer glasses, J. Chem. Phys. **128**, 134902 (2008).
[31] H. N. Lee, R. A. Riggleman, J. J. de Pablo, and M. Ediger, Deformation-induced mobility in polymer glasses during multistep creep experiments and simulations, Macromolecules **42**, 4328 (2009).
[32] R. Pérez Aparicio, D. Cottinet, C. Crauste Thibierge, L. Vanel, P. Sotta, J. Y. Delannoy, D. R. Long, and S. Ciliberto, Dielectric spectroscopy of a stretched polymer glass: Heterogeneous dynamics and plasticity, Macromolecules **49**, 3889 (2016).
[33] R. Sahli, J. Hem, C. Crauste Thibierge, F. Clément, D. Long, and S. Ciliberto, Relaxation time of a polymer glass stretched at very large strains, Phys. Rev. Mater. **4**, 035601 (2020).
[34] O. Narayanaswamy, A model of structural relaxation in glass, J. Am. Ceram. Soc. **54**, 491 (1971).
[35] B. Riechers, L. A. Roed, S. Mehri, T. S. Ingebrigtsen, T. Hecksher, J. C. Dyre, and K. Niss, Predicting nonlinear physical aging of glasses from equilibrium relaxation via the material time, Sci. Adv. **8**, eabl9809 (2022).
[36] See Supplemental Material at http://link.aps.org/supplemental/10.1103/PhysRevLett.132.208101 for additional experimental details and Chen and Schweizer model calculations, which includes Refs. [37–41].
[37] H. N. Lee, K. Paeng, S. F. Swallen, and M. Ediger, Direct measurement of molecular mobility in actively deformed polymer glasses, Science **323**, 231 (2009).
[38] B. Bending, K. Christison, J. Ricci, and M. Ediger, Measurement of segmental mobility during constant strain rate deformation of a poly(methylmethacrylate) glass, Macromolecules **47**, 800 (2014).
[39] J. Ricci, T. Bennin, and M. Ediger, Direct comparison of probe reorientation and linear mechanical measurements of segmental dynamics in glassy poly(methyl methacrylate), Macromolecules **51**, 7785 (2018).
[40] K. Chen and K. S. Schweizer, Theory of aging, rejuvenation, and the nonequilibrium steady state in deformed polymer glasses, Phys. Rev. E **82**, 041804 (2010).
[41] J. Schindelin, I. Arganda Carreras, E. Frise, V. Kaynig, M. Longair, T. Pietzsch, S. Preibisch, C. Rueden, S. Saalfeld, and B. Schmid, Fiji: An open-source platform for biological-image analysis, Nat. Methods **9**, 676 (2012).
[42] M. D. Ediger, Spatially heterogeneous dynamics in supercooled liquids, Annu. Rev. Phys. Chem. **51**, 99 (2000).
[43] H. N. Lee and M. Ediger, Mechanical rejuvenation in poly (methylmethacrylate) glasses? Molecular mobility after deformation, Macromolecules **43**, 5863 (2010).
[44] K. Hebert, B. Bending, J. Ricci, and M. Ediger, Effect of temperature on postyield segmental dynamics of poly (methylmethacrylate) glasses: Thermally activated transitions are important, Macromolecules **48**, 6736 (2015).
[45] K. Chen and K. S. Schweizer, Molecular theory of physical aging in polymer glasses, Phys. Rev. Lett. **98**, 167802 (2007).
[46] K. Chen and K. S. Schweizer, Microscopic constitutive equation theory for the nonlinear mechanical response of polymer glasses, Macromolecules **41**, 5908 (2008).
[47] K. Chen and K. S. Schweizer, Theory of yielding, strain softening, and steady plastic flow in polymer glasses under constant strain rate deformation, Macromolecules **44**, 3988 (2011).
[48] G. A. Medvedev, E. Xing, M. D. Ediger, and J. M. Caruthers, Multistep deformation experiment and development of a model for the mechanical behavior of polymeric glasses, Macromolecules **55**, 6351 (2022).
[49] A. Ghosh and K. S. Schweizer, The role of collective elasticity on activated structural relaxation, yielding, and steady state flow in hard sphere fluids and colloidal suspensions under strong deformation, J. Chem. Phys. **153**, 194502 (2020).